ISSN 1027-5495. Functional Materials, 32, No.4 (2025), p. 578-585
doi:http://dx.doi.org/10.15407/fm32.04.578

Investigation of properties and structure of polymer coatings based on epoxy polymer and trimethoprim

O.O. Sapronov[1], V.L. Demchenko[2], V.D. Sharanov[1], D.O. Danylenko[1], A.V. Sapronova[1], V.V. Sotsenko[1], P.O. Vorobiov[1], K.Yu. Yurenin[1], P.P. Fostyk[1], M.M. Banha[1], I.O. Sytnyk[2]

[1]Kherson State Maritime Academy, 20 Ushakov Ave., Kherson, 73009, Ukraine
[2]E.O. Paton Electric Welding Institute of the National Academy of Sciences of Ukraine, 11 Kazymyr Malevich St., Kyiv, 03150, Ukraine

Received March 19, 2025

The properties and structure of composites based on epoxy polymer and the synthetic antibiotic trimethoprim were investigated. It was found that the dispersed filler trimethoprim $C_{14}H_{18}N_4O_3$ exhibited an amorphous structure in the volume of the epoxy polymer, partially post-curing the polymer matrix. The introduction of trimethoprim into the epoxy matrix at a content of q = 10-15 wt.%. makes it possible to obtain new polymeric materials with improved mechanical properties, in particular: the flexural elastic modulus increases from E = 2.90 GPa to E = 3.67 GPa; the impact strength increases from W = 7.0 kJ/m^2 to W = 12.8 kJ/m^2; the flexural strength increases from σ_b = 48.0 MPa to σ_b = 87.7 MPa compared to the original epoxy composite. The change in the morphology of the epoxy polymer upon the introduction of an active filler was studied by optical microscopy. Based on the analysis of infrared spectra in the wavenumber range v = 900-4000 cm^{-1}, structural changes in the studied materials were determined, indicating the chemical interaction of the antibiotic with the epoxy polymer. X-ray diffraction analysis showed that the initial dispersed filler trimethoprim has a crystalline structure, and the epoxy polymer filled with trimethoprim has an amorphous structure. This may indicate the dissolution of the filler in the volume of the epoxy polymer.

Keywords: epoxy binder; amine hardener; active filler; physical and mechanical properties; structure

Дослідження властивостей і структури полімерних покриттів на основі епоксидного полімеру і триметоприму. *О.О. Сапронов, В.Л. Демченко, В.Д. Шаранов, Д.О. Даниленко, А.В. Сапронова, В.В. Соценко, П.О. Воробйов, К.Ю. Юренін, П.П. Фостик, М.М. Банга, І.О. Ситник*

У роботі досліджено властивості та структуру композитів на основі епоксидного полімеру і синтетичного антибіотика – триметоприму. Встановлено, що дисперсний наповнювач триметоприм $C_{14}H_{18}N_4O_3$ проявляв аморфну структуру у об'ємі епоксидного полімеру, частково доотверджуючи полімерну матрицю. Введення у епоксидну матрицю триметоприму за вмісту q = 10-15 мас. ч. дозволяє отримати нові полімерні матеріали з підвищеними механічними властивостями, зокрема: модуль пружності при згинанні зростає з E = 2,90 ГПа до E = 3,67 ГПа; ударна в'язкість зростає з W = 7,0 кДж/м^2 до W = 12,8 кДж/м^2; межа міцності при згинанні зростає з σ_b = 48,0 МПа до σ_b = 87,7 МПа порівняно з вихідним епоксидним композитом. Методом оптичної мікроскопії досліджено зміну морфології епоксидного полімеру при введенні активного наповнювача. На основі аналізу ІЧ-спектрів у області хвильових чисел v = 900…4000 cm^{-1} були встановлені структурні зміни досліджуваних матеріалів, що вказують на хімічну взаємодію антибіотику з епоксидним полімером. Методом рентгеноструктурного аналізу було встановлено, що вихідний дисперсний наповнювач триметоприм характеризується кристалічною структурою, а епоксидний полімер наповнений триметопримом має аморфну структуру. Це може свідчити про розчинення наповнювача в об'ємі епоксидного полімеру.

1. Introduction

Marine navigation equipment includes a range of tools and systems designed for navigation at sea and efficient ship management during operation. The surfaces of such structures are exposed to moisture and contamination, which is the root cause of corrosion processes. For deck equipment, particularly navigation equipment, the electrochemical process of corrosion destruction prevails [1-3]. The electrochemical process involves the presence of cathodic and anodic areas on the corroded surface and an electrolyte, a film of moisture from sea water or atmospheric air condensate. Such moisture films can contain gases, such as carbon dioxide (CO_2), sulfur dioxide (SO_2), sulfur trioxide (SO_3), and nitrogen dioxide (NO_2), which are soluble in air. It should be noted that a moisture film is constantly present on the metal surface of marine navigation equipment. Since global communication is crucial for shipping, as it affects the timing of cargo delivery by waterways, it is essential to ensure the reliability of radar systems. For this purpose, surface protection of navigation equipment is used by applying protective epoxy coatings [4-6]. Their use is due to high adhesive and physico-mechanical properties, low density, resistance to aggressive external factors, and durability [7-17]. At the same time, the strengthening in global trade and economic restrictions on the use of coatings containing biocides [18-20] is encouraging the search and development of new environmentally friendly alternatives. Thus, the authors of [21, 22] proposed using polymeric superhydrophobic nanocomposites based on polysiloxane. An inorganic -Si-O bond in the polymer structure provides minimal adhesion to external contaminants, including marine microorganisms. However, the main disadvantage is the low mechanical characteristics of such materials [23]. The authors of [15] showed that combining nanoscale and microscale additives in a polymer binder allows for targeted control of the structure of coatings. Such an approach ensures the formation of a porous nano heterogeneous coating structure, which leads to an accelerated release of silver ions from the polymer surface and inhibition of the process of fouling metal structures. However, the cost of nanodispersed silver limits the use of such coatings.

This work aims to study the effect of the optimal content of the dispersed filler trimethoprim on the physico-mechanical properties and structure of epoxy coatings, as well as to develop a structural model of the interaction of the ingredients used.

2. Materials and methods

The following components were used to create polymer coatings to protect the surfaces of metal structures: binder – epoxy oligomer ED-20; hardener – polyethylene polyamine (PEPA); ratio of the components (wt.%) – ED-20: PEPA – 100 : 10.

To improve the properties of the epoxy polymer, a dispersed filler trimethoprim $C_{14}H_{18}N_4O_3$ (TMP) (CAS: 738-70-5, China) in the form of a yellow crystalline substance was used. TMP is a synthetic antibiotic capable of inhibiting microorganisms and bacteria (Fig. 1). TNP particles have a size of 5-10 microns.

The coating formation was carried out in a certain sequence, according to the technology described in [24-27].

The tensile strength and flexural modulus were determined according to ASTM D790-03. Specimen parameters: length l = 120 ± 2 mm, width b = 15 ± 0.5 mm, height h = 10 ± 0.5 mm.

The impact strength was determined according to ASTM D6110-18 on a pendulum tester MK-30 at a temperature of T = 298 ± 2 K and relative humidity d = 50 ± 5 %. Samples with dimensions of (63.5 × 12.7 × 12.7) ± 0.5 mm were used.

The morphology of the composites was studied using a Versamet 2 microscope [28].

The interaction of components in the studied samples was identified by FTIR absorption spectroscopy using a Fourier transform spectrophotometer "Tenzor-37" (BRUKER, Germany) in the frequency range $\nu = 500 \div 4000$ cm^{-1}.

The features of the structural organization of epoxy polymer-based composites were studied by wide-angle X-ray diffraction using an XRD-7000 diffractometer (Shimadzu, Japan); the X-ray optical scheme was implemented using the Debye-Scherrer method for passing the

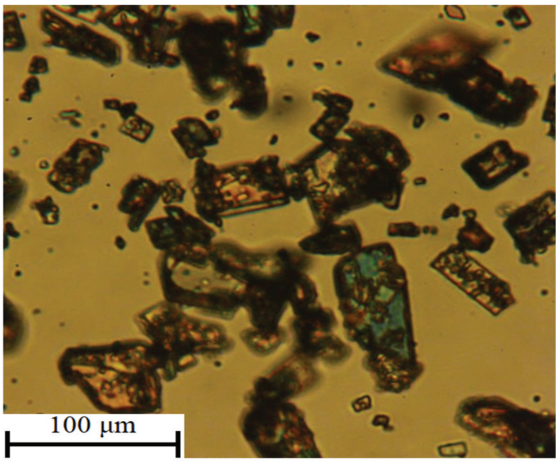

a

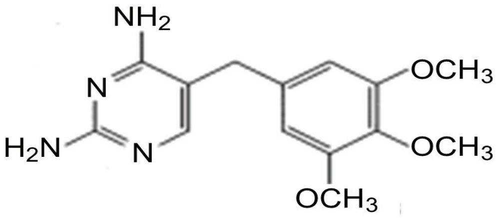

b

Fig. 1 Dispersed filler trimethoprim $C_{14}H_{18}N_4O_3$: a) – general view obtained by optical microscopy; b) – structural formula of trimethoprim $C_{14}H_{18}N_4O_3$

primary beam through the sample under study; CuK_α- radiation (λ = 1.54 Å) and a graphite monochromator were used [29, 30]. The measurements were performed by automatic stepwise scanning in the mode U = 30 kB, I = 30 mA in the range of scattering angles (2θ) from 3.0 to 40 degrees. The exposure time was 5 s. The temperature of the study was T = 293 ± 2 K.

3. Results and discussion

To determine the optimal content of the dispersed filler, trimethoprim $C_{14}H_{18}N_4O_3$, in the epoxy binder ED-20, comprehensive studies of the physical and mechanical properties and structure of polymers were carried out. It was experimentally established (Fig. 2) that the introduction of trimethoprim into the polymer binder at a content of q = 5.0 wt.% increases the flexural elastic modulus from E = 2.9 GPa (unfilled polymer) to E = 3.0 GPa and the impact strength from W = 7.0 kJ/m^2 to W = 9.0 kJ/m^2. The analysis of the polymer fracture surface (Fig. 3, a) revealed a relief surface structure with dark spots. An increase in the content of the dispersed filler to q = 10.0 wt.% leads to the formation of a composite with a bending elastic modulus of E = 3.67 GPa.

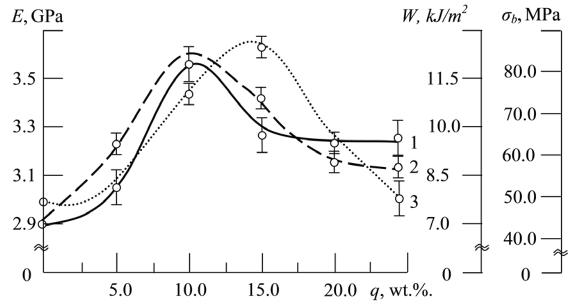

Fig. 2. Dependence of the flexural elastic modulus (E), impact strength (W), and fracture stresses in bending (σ_b) of polymeric materials on the content of $C_{14}H_{18}N_4O_3$ filler: 1 – flexural elastic modulus (E); 2 – impact strength (W); 3 – flexural strength (σ_b).

A similar result was observed for the impact strength of the filled polymer, W = 12.8 kJ/m^2. It was assumed that by introducing the optimal filler content and the effect of ultrasonic dispersion of the composition, conditions are created for a uniform spatial distribution of the filler in the polymer binder. At the same time, analyzing the fracture surface of the studied polymeric materials (Fig. 3, b) allowed us to identify similar dark spots with a total area larger than the base material. This may indicate the solubility of the filler in the polymer matrix. At the same time, we do not observe the presence of crack propagation lines around these dark spots (Fig. 3, d, e). New structures (dark spots) are formed, differing from the main ones, characterized by increased adhesion strength at the polymer-filler interface. This inhibits the crack propagation in the polymer.

Introducing $C_{14}H_{18}N_4O_3$ at a content of q = 15.0 wt.% leads to a partial decrease in the flexural elastic modulus (E = 3.3 GPa) and impact strength (W = 11.0 kJ/m^2). However, the tensile strength of the samples in flexure reaches a maximum value of σ_b = 87.7 MPa. This result can be explained as the optimization of the content of the active filler trimethoprim, which creates conditions for the compaction of the polymer structure (Fig. 3, c).

At the same time, a more viscous fracture pattern was observed, improving the tensile strength. The further introduction of trimethoprim $C_{14}H_{18}N_4O_3$ (q = 20.0-25.0 wt.%) leads to a deterioration in the strength characteristics of the polymeric materials under study (Fig. 2). This may be due to the oversaturation of the composition with trimethoprim, which leads to the formation of structural defects in the form of particle aggregates in the polymer volume (Fig. 3, d, e).

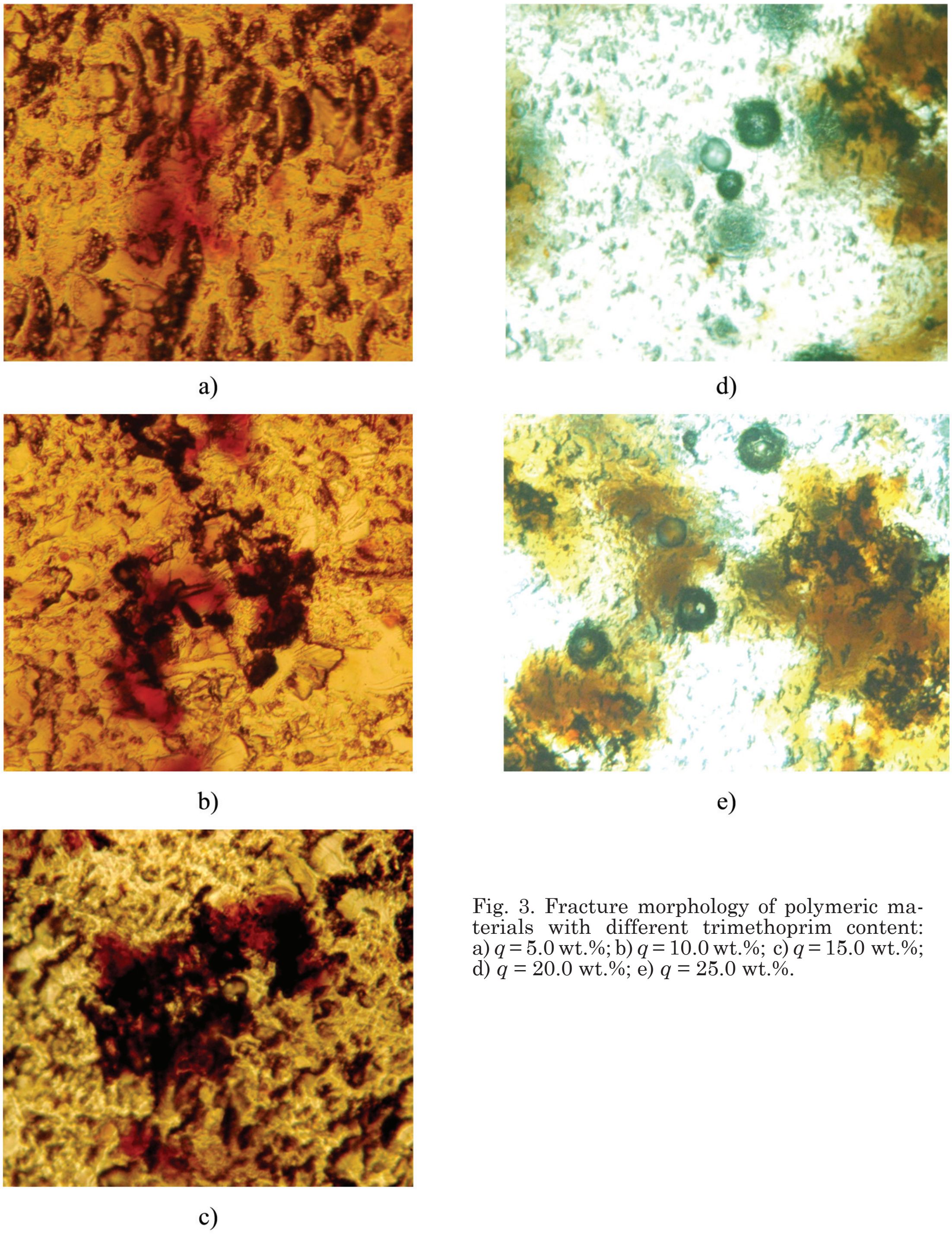

Fig. 3. Fracture morphology of polymeric materials with different trimethoprim content: a) $q = 5.0$ wt.%; b) $q = 10.0$ wt.%; c) $q = 15.0$ wt.%; d) $q = 20.0$ wt.%; e) $q = 25.0$ wt.%.

The next step was to study the epoxy composites by IR spectroscopy. The samples used for the study were: 1) trimethoprim dispersed filler powder; 2) ED-20 epoxy resin; 3) ED-20 + 10 wt.% trimethoprim; 4) ED-20 + 30 wt.% trimethoprim. Samples 3 and 4 were prepared under conditions similar to the preparation of ED-20 - PEPA polymer systems, i.e., preliminary polymerization was performed at room temperature $T = 293$ K for 12 hours, followed by heat treatment at $T = 393$ K for 2 hours.

Based on the analysis of the works [31-33], it was found that epoxy -C-O-C- groups can be observed at $\nu = 915\text{-}920$ cm^{-1}, as well as at higher wavenumbers, in particular, $\nu = 4530$ cm^{-1}. The authors of [34] noted that a decrease in intensity (T, %) and, accordingly, the relative peak

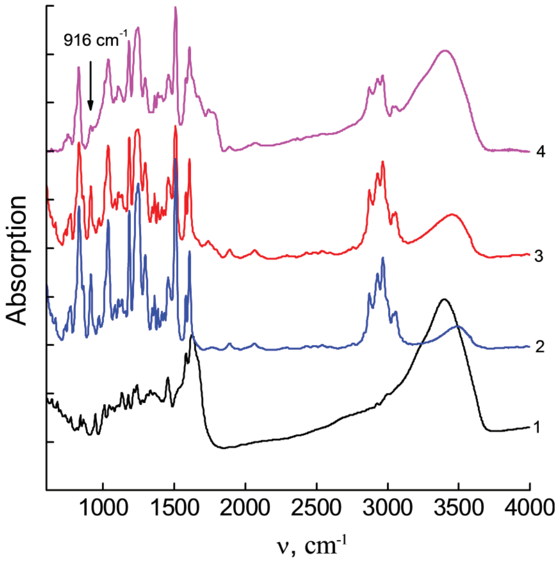

Fig. 4. Infrared spectra: 1. trimethoprim ($C_{14}H_{18}N_4O_3$); 2. ED-20; 3. ED-20 + 10 wt.% trimethoprim; 4. ED-20 + 30 wt.% of trimethoprim.

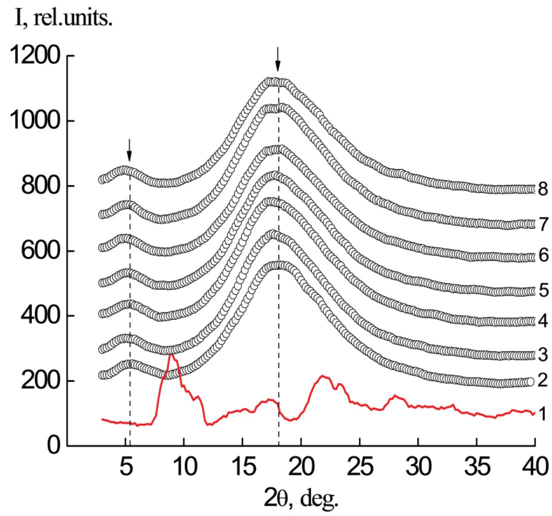

Fig. 5. Wide-angle X-ray diffraction patterns of samples of filler (trimethoprim) (1); the original epoxy polymer (2); epoxy polymer with different content of trimethoprim $C_{14}H_{18}N_4O_3$: 5.0 wt.% (3), 10.0 wt.% (4), 15.0 wt.% (5), 20.0 wt.% (6), 25.0 wt.% (7), 30.0 wt.% (8).

area (S, %) indicates the opening of the epoxy group during thermal crosslinking.

Thus, a comparative analysis of the IR spectra (Fig. 4) showed a slight decrease in the peak intensity at a wavenumber ν = 916 cm^{-1} for the ED-20-based sample containing 10 wt.% trimethoprim. For the sample ED-20 + 30 wt.% trimethoprim, the peak at ν = 916 cm^{-1} is almost absent. This indicates that the dispersed filler trimethoprim reacts with the epoxy resin and cures it.

In the studied ED-20 – PEPA – trimethoprim composites, the dispersed filler acts as a post-curing agent for the polymer matrix.

The analysis of the wide-angle X-ray diffraction pattern of trimethoprim $C_{14}H_{18}N_4O_3$ introduced into the epoxy polymer (Fig. 5, curve 1) showed that it has a crystalline structure (due to a significant number of diffraction maxima). In contrast, the starting polymer, i.e., the epoxy matrix, has an amorphous structure (Fig. 5, curve 2). According to the ratio of ED-20 and PEPA used to obtain the mesh polymer (Fig. 5, curve 2), the higher intensity diffraction maximum ($2\theta_{max} \approx 18{,}1^o$) indicates the presence of short-range order during the translation in space of fragments of internodal molecular links of ED-20, and the secondary intensity maximum ($2\theta_{max} \approx 5{,}4^o$) belongs to PEPA. The average value of the period d of short-range ordering of both types of internodal molecular links (the average distance between the layers of these links equal to 4.89 Å and 16.34 Å, respectively, in the polymer volume) was determined according to the Bragg equation:

$$d = \lambda(2\sin\theta_m)^{-1},$$

where λ is the wavelength of the characteristic X-ray radiation (λ = 1.54 Å for Cu*K*α radiation).

When trimethoprim $C_{14}H_{18}N_4O_3$ was added to the epoxy polymer at 5.0 wt.%, we observed a shift of the amorphous halo, which characterizes the features of the ED-20 structure, to the region of smaller angles: from $2\theta_{max} \approx 18.1^o$ (for unfilled epoxy polymer) to $2\theta_{max} \approx 17.6^o$ (for epoxy polymer containing q = 5.0 wt.% filler) (Fig. 5, curves 2, 3). This indicates that when the filler is introduced into the epoxy matrix, the average Bragg distance between the layers of ES molecular units increases from $d \approx 4.89$ Å to $d \approx 5.03$ Å.

It should be noted that an increase in the filler content in the volume of the polymer matrix to q = 10.0 wt.% leads to a further rise in the Bragg distance between the molecular chains of ED-20 (Fig. 6). This result can be explained by the fact that, at a relatively low content, the filler actively interacts with the polymer matrix and is evenly distributed throughout its volume. With an increase in the filler content to q = 15.0-25.0 wt.%, the value of d decreases slightly and remains unchanged (Fig. 6). At the highest filler content in the epoxy matrix (q = 30.0 wt.%), the Bragg distance between the macromolecular chains of the epoxy matrix decreases sharply, which may be due to the ag-

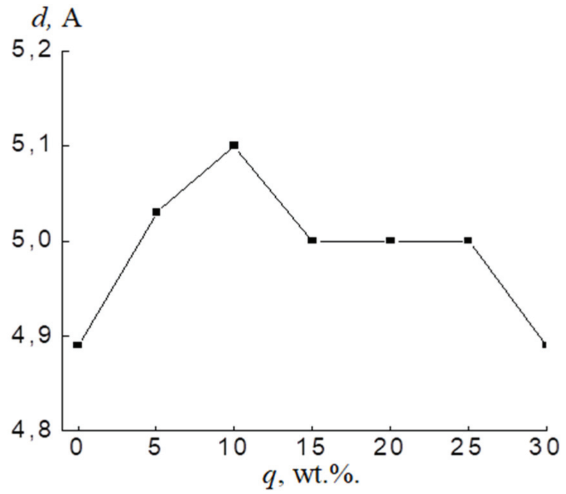

Fig. 6. Bragg distance between the layers of ES molecular links depending on the filler content in the polymer matrix.

gregation of the filler in the polymer. The data obtained are consistent with the results of the study of physical and mechanical properties and optical microscopy.

It should be noted that when trimethoprim is introduced into the epoxy matrix, its crystal structure does not appear in the volume of the composite. This may indicate that the filler is dissolved in the composite and participates in the final curing of the samples.

Table 1 shows the values of the Bragg distance between the molecular units of the studied samples.

A comprehensive analysis of the structure of the studied polymer materials using modern research methods (IR spectral analysis, X-ray structural analysis), allows us to confirm the amorphous structure of the filler in the composites (dissolution of the filler in the volume of the epoxy polymer) and the participation of primary amino groups (NH_2) of trimethoprim in the process of thermal crosslinking of ED-20, which ensures the post-curing of the epoxy polymer with the formation of a new structure.

Thus, the obtained research results make it possible to propose a structural and molecular model (Fig. 7, 8) of the interaction of the ingredients of the polymer coating. From the structural and molecular model, it is clear that the interaction of the ingredients of the polymer coating occurs with the participation of the primary amino groups of trimethoprim, the opening of the epoxy ring and the subsequent crosslinking of the epoxy polymer.

4. Conclusions

According to the results of comprehensive studies of the physical-mechanical properties and structure of epoxy composites, it was found that the optimal content of the filler (trimethoprim) $C_{14}H_{18}N_4O_3$ in the polymer matrix is q = 10.0-15.0 wt.%. The rational content of the antibiotic in the epoxy binder changes the structure of the materials. When the filler is introduced into the epoxy matrix, the average Bragg distance between the macromolecular chains of the epoxy polymer changes.

The chemical interaction of trimethoprim $C_{14}H_{18}N_4O_3$ particles with the macromolecular chains of the epoxy binder ED-20 was investigated using the IR spectral analysis method. A decrease in the peak intensity at ν = 916 cm-1 was established with an increase in the antibiotic content in the epoxy matrix. The study results show that the filler with active primary amino groups (NH_2) can provide additional post-curing of the polymer matrix. At the same time, the mechanical strength of the developed coatings increases, in particular: the modulus of elasticity in bending increases from $E = 2.90$ GPa to $E = 3.67$ GPa; the impact strength increases from $W = 7.0$ kJ/m^2 to $W = 12.8$ kJ/m^2; the ultimate bending strength increases from σ_b = 48.0 MPa to σ_b = 87.7 MPa.

Using the wide-angle XRD, it was established that the dispersed filler trimethoprim

Table 1. Bragg distance between molecular links of the samples

Filler content in the volume of the epoxy matrix, wt. %.	2θm, deg. (ED-20)	d, Å (ED-20)	2θm, deg. (PEPA)	d, Å (PEPA)
0	18.1	4.89	5.4	16.34
5.0	17.6	5.03	5.4	16.34
10.0	17.3	5.10	5.4	16.34
15.0	17.8	5.00	5.2	16.97
20.0	17.8	5.00	5.2	16.97
25.0	17.8	5.00	5.2	16.97
30.0	18.1	4.89	5.0	17.70

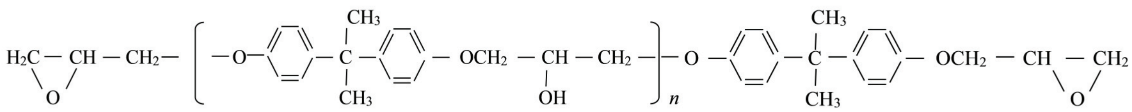

a)

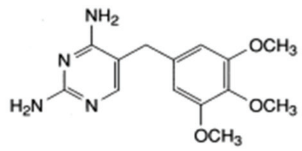

b)

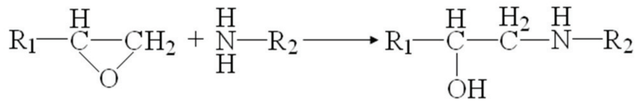

c)

Fig. 7. Structural model of the interaction of the ingredients of the developed polymer coating: *a* – structural formula of the epoxy oligomer ED-20; *b* – structural formula of the filler trimethoprim $C_{14}H_{18}N_4O_3$; *c* – structural formula of the interaction of the ingredients of the polymer coating.

$C_{14}H_{18}N_4O_3$ has a crystalline structure. The analysis of the diffraction patterns of the studied samples showed that the filler introduced into the polymer matrix in a wide concentration range (q = 5.0-30.0 wt.%) does not exhibit its crystalline structure. The obtained result may indicate the dissolution of the filler in the volume of the epoxy polymer and the chemical interaction of trimethoprim with the polymer matrix. That is, a competing reaction of the interaction of the antibiotic and hardener with the epoxy binder may occur, which increases the degree of crosslinking of the polymer coating.

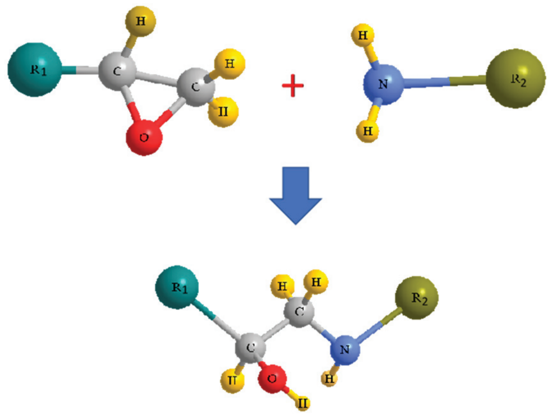

Fig. 8. Molecular model of the interaction of the ingredients of the developed polymer coating.

References

1. M. Feng, S.-L. Shaw, G. Peng, Z. Fang, *J. Transp. Geogr.,* **86** (2020).
2. B. Mei, L. Sun, G. Shi, *Sensors 2020*. **20**, 3963 (2020).
3. A. Buketov, O. Sapronov, M. Brailo, et al., *Adv. in Mater. Science and Engineering*. 2019. 8183761 (2019).
4. L. Tan, *China Strategic Emerging Industry*, **10**, 0149 (2019).
5. J. Zhang, S. Jia, X. Wang, et al., *New Technology and New Products in China*, **15**, 80 (2022).
6. H. Zhao, W. Zhao, X. Zhang, *Fujian Chemical Industry*, **10**, 135 (2013).
7. A. Buketov, O. Sapronov, K. Klevtsov, B. Kim, Polymers, **15**, 3449 (2023).
8. O.V. Totosko, P.D. Stukhlyak, A.H. Mykytyshyn et al., *Funct. Mater.,* **27**, 760 (2020).
9. O. Sapronov, P. Maruschak, V. Sotsenko et al., *J. Mar. Sci. Eng*., **8**, 527 (2020).
10. I.G. Dobrotvor, P.D. Stukhlyak, A.G. Mykytyshyn et al., *Strength Mater*, **53**, 283 (2021).
11. O.O. Sapronov, A.V. Buketov, D.O. Zinchenko, V.M. Yatsyuk, *Composites: Mechan. Computat., Applicat.*, **8**, 47 (2017).
12. N. Dolgov, P. Stukhlyak, O. Totosko et al., *Mechanics of Advanced Materials and Structure*, **1** (2023).
13. A.V. Buketov, N.A. Dolgov, A.A. Sapronov et al., *Strength of Mater.*, **50**, 425 (2018).
14. E.A. Lysenkov, O.V. Stryutskiy, Yu.P.Gomza, V.V. Klepko, *Funct. Mater.,* **22**, 40 (2015).
15. O.Sapronov, A. Buketov, B. Kim, P. Vorobiov, L. Sapronova, *Materials,* **17**, 1503 (2024).
16. V. Kashytskyi, P. Savchuk, V. Malets et al., *Eastern-Europ. J. of Enterp. Technolog.,* **3**, 16 (2017).

17. A.V. Buketov, O.O. Sapronov, M.V.Brailo, *Strength of Materials*, **46**, 717 (2014).
18. M.S. Selim, S.A. El-Safty, M.A. El-Sockary, et al., *Materials & Design*, **101**, 218 (2016).
19. Y. Vystavna, Z. Frkova, H. Celle-Jeanton, et al., *Sci. Total Environ*, **637**, 1358 (2018).
20. A. Panda, K. Dyadyura, J. Valíček, et al., Polymers, **14**, 3275 (2022).
21. M.S. Selim, S.A. El-Safty, M.A. Shenashen, *Superhydrophobic Polymer Coatings*, **181**, 203 (2019).
22. Diego Meseguer Yebra, Søren Kiil, Kim Dam-Johansen, *Progress in Organic Coatings*, 50, 75 (2004).
23. S.S. Mohamed, M.A. Ahmed, A.H. Shimaa, et al., *Chemical Engineering Science*, **291** (2024).
24. A. Buketov, P. Maruschak, O. Sapronov et al., *Mol. Liq. Cryst.*, **628**, 167 (2016).
25. A. Buketov, O. Sapronov, A. Menou, et al., *Transbaltica 2021*, **F1395**, 212 (2022).
26. P.O. Maruschak, M.V. Kindrachuk, I.A. Sieliverstov, et al., *Funct. Mater.,* **31,** 26 (2024).
27. O.O. Sapronov, A.V. Buketov, S.V. Yakushchenko et al., *Composites: Mechan. Computat., Applicat.,* **12** , 23 (2021).
28. O. Masiuchok, M. Iurzhenko, R. Kolisnyk, et al., *Polymers*, **14**, 4022 (2022).
29. V.L. Demchenko, V.I. Shtompel, S.V. Riabov, *Polymer Science*, **57**, 635 (2015).
30. V.L. Demchenko, S.M. Kobylinskyi, S.V. Riabov, et al., Applied Nanoscience, **10**, 5409 (2020).
31. G. Nikolic, S. Zlatkovic, M. Cakic, *Sensors*, **10**, 684 (2010).
32. C. S. Chen, B. J. Bulkin, E. M. Pearce, *Journal of Applied Polymer Science,* **28**, 1077 (1983).
33. J. Mijovic, S. Andjelic, *Macromolecules,* **28**, 2787 (1995).
34. R. Hardis, J.L.P. Jessop, F.E. Peters, M.R. Kessler, *Composites Part A,* **49,** 100 (2013).